

Original Article

Cite this article: Bezerra FI, da Silva JH, Agressot EVH, Freire PTC, Viana BC, and Mendes M (2023) Effects of chemical weathering on the exceptional preservation of mineralized insects from the Crato Formation, Cretaceous of Brazil: implications for late diagenesis of fine-grained *Lagerstätten* deposits. *Geological Magazine* **160**: 911–926. <https://doi.org/10.1017/S0016756823000043>

Received: 4 August 2022
Revised: 13 January 2023
Accepted: 16 January 2023
First published online: 1 March 2023


Keywords:

taphonomy; mineralization; *in situ* weathering; pseudomorphism; oxidation; post-diagenesis; palaeontological information

Author for correspondence:

Francisco Irineudo Bezerra,
Email: irineudoufc@gmail.com

Effects of chemical weathering on the exceptional preservation of mineralized insects from the Crato Formation, Cretaceous of Brazil: implications for late diagenesis of fine-grained *Lagerstätten* deposits

Francisco Irineudo Bezerra¹ , João Hermínio da Silva²,
Enzo Victorino Hernández Agressot³, Paulo Tarso C. Freire⁴,
Bartolomeu Cruz Viana⁵ and Márcio Mendes¹

¹Programa de Pós-graduação em Geologia, Universidade Federal do Ceará, Fortaleza, Ceará 64049-550, Brazil; ²Centro de Ciências e Tecnologia, Universidade Federal do Cariri, Juazeiro do Norte, Ceará 63048-080, Brazil; ³Campus Foz do Iguacu, Instituto Federal do Paraná, Foz do Iguacu, Paraná 85860-000, Brazil; ⁴Programa de Pós-graduação em Física, Universidade Federal do Ceará, Fortaleza, Ceará 60455-970, Brazil and ⁵Laboratório interdisciplinar de materiais avançados, Universidade Federal do Piauí, Teresina, Piauí 64049-550, Brazil

Abstract

Many studies have improved our understanding of the mode of preservation at the Crato fossil *Lagerstätte*. The high degree of preservation of the Crato mineralized insects is thought to be a consequence of the diffusion of ions through carcasses and envelopment by bacteria that, in turn, created microenvironmental conditions that led to mineralization, mainly pyritization. Pyritized insects have been oxidized by *in situ* weathering to more stable oxide/hydroxy minerals during Quaternary time. This transformation is essential to maintain the palaeontological information acquired during microbially induced pyritization in an oxidizing atmosphere. However, intense weathering can diminish or obscure the morphological fidelity, and little attention has been paid to the post-diagenetic processes experienced by these fossils. Here, we aim to determine the degree of alteration undergone by Crato pyritized insects using the following combination of analytical tools: scanning electron microscopy, energy dispersive X-ray spectroscopy, Fourier transform infrared and Raman spectroscopy. Our results show that well-preserved insects are preferentially replaced by haematite and poorly preserved fossils are replaced by goethite. In addition, we recorded three types of post-diagenetic alteration: insects with iron-oxide overgrowths; insects associated with black coatings, sometimes with the formation of dendrites; and insects preserved as an impression, where only the outline of the body remains. All of these alterations have the potential to distort or tarnish palaeontological information. Here, we measured the effects of such telodiagenetic alterations at macro and micro scales. Therefore, this taphonomic approach has wide applicability wherever fine-grained deposits bearing mineralized insects are found.

1. Introduction

Over the past few years, our knowledge of fossil insects has increased exponentially. Studies focusing on behavioural advances, eusociality, plant–insect interactions, extinction–origination rates and biostratigraphic issues have helped us to understand why insects have the highest described species-level diversity we find today (Clapham & Karr, 2012; Karr & Clapham, 2015; Nicholson *et al.* 2015; Clapham *et al.* 2016; Labandeira *et al.* 2016; Labandeira, 2019; Barden & Engel, 2021). Although insects have a rich fossil record, they contain large temporal and taxonomic gaps in their evolutionary history (Schachat & Labandeira, 2021). This is due to the overwhelming majority of described insect fossils coming from fossil *Lagerstätte* assemblages. Insect assemblages embedded in *Lagerstätten*-type deposits allow a vast number of specimens to be collected (*Konzentrat Lagerstätten*), and they often exhibit exceptionally well-preserved insects (*Konservat-Lagerstätten*). Fossil insects in the *Lagerstätte* assemblages are generally preserved in lacustrine or amber deposits. For lacustrine deposits, insects are usually preserved as fossil compressions via mineralization. As an example, one of the best-studied *Lagerstätten* bearing insects is the Green River Formation from the Piceance Creek Basin in Colorado. After a thorough study was carried out in this unit, Anderson & Smith (2017) reported that insects are typically preserved by haematite after pyrite and as carbonaceous compressions, both preservational modes having a high fidelity of anatomical detail for individual body parts. The Jehol biota in northeastern China also hosts a significant palaeoentomofauna in

a freshwater deposit with volcanogenic sediments. Wang *et al.* (2012) observed that many insects in the Jehol biota were preserved by framboids and microcrystalline pyrite.

The excessive attention given to the insects encountered in *Konservat-Lagerstätten* localities has given rise to the interest of many researchers in unravelling the taphonomic causes of this preservation in fine detail. The taphonomy of a fossil can be divided into three stages: biostratinomy, diagenesis and recovery (Donovan, 1991; Henwood, 1993). According to Henwood (1992, 1993), biostratinomy and recovery probably have substantially more taphonomic influence than diagenesis for insects preserved in amber inclusions. For those preserved in lacustrine deposits, diagenesis seems to stand out as the most relevant stage. More and more palaeoentomologists have invested in taphonomic investigations, and most of these studies focus on biostratinomic events and/or early–middle diagenetic processes (Duncan & Briggs, 1996; Zhehikhin, 2002; Martínez-Delclòs *et al.* 2004; Smith *et al.* 2006; Smith & Moe-Hoffman, 2007; McNamara *et al.* 2011, 2012; Smith, 2012; Thoene-Henning *et al.* 2012; Wang *et al.* 2012; McNamara, 2013; Pan *et al.* 2014; Greenwalt *et al.* 2015; Anderson & Smith, 2017; Tian *et al.* 2020; Iniesto *et al.* 2021; Heingård *et al.* 2022).

The Crato palaeoentomofauna, from the Aptian of northeastern Brazil, is perhaps the most studied palaeoentomofauna preserved in fine carbonate strata in the world. Crato insects are commonly complete and three-dimensionally preserved, revealing characteristics such as abdominal segmentation, wings displaying well-defined venation and head appendages. A consequence of this exceptional preservation is that the majority of studies on the Crato palaeoentomofauna are focused on taxonomic and evolutionary issues. However, an increasing number of investigations have analysed the general insect taphonomy, with a focus on early-diagenetic issues (Delgado *et al.* 2014; Barling *et al.* 2015, 2020, 2021; Osés *et al.* 2016; Bezerra *et al.* 2018, 2020, 2021; Dias & Carvalho, 2020, 2021; Prado *et al.* 2021). These authors briefly mentioned the effect of weathering. The high degree of fidelity of the Crato insects was achieved during early-mesodiagenesis under reducing conditions mediated by microbial mats (Osés *et al.* 2016; Varejão *et al.* 2019; Dias & Carvalho, 2021). After final burial, ions and sulfate-reducing bacteria favour the formation of framboidal pyrite, which replaces cuticle and labile tissues and prevents the total collapse of the carcass. Then, telodiagenetic processes transform the pyritized replicas into more stable minerals as the specimens approach atmospheric conditions by denudation of the rock package. This process, under certain circumstances, ensures that the morphological information acquired during early diagenesis survives oxidizing agents and reaches today's palaeoentomologists. However, the weathering of fossils has the potential to lead to taphonomic consequences, including loss of morphological information. This process can make the weathered specimen unsuitable for systematic studies, which may induce palaeoentomologists/researchers to become disinterested in collecting these specimens during field campaigns. Under extreme conditions, intense weathering can leach away the fossil insect without leaving any evidence of its existence. McNamara *et al.* (2012) recognized that the exceptionally preserved characters of the cuticle layers, as well as the insect staining pattern are directly associated with a low rate of chemical weathering.

In this study, we do not consider telodiagenetic effects a part of the fine-scale preservation process. Rather, we suggest that late diagenesis limits preservation potential. To address the lack of information about telodiagenetic processes we integrate mineralogical,

chemical and spectroscopic data to identify the post-diagenetic alterations affecting mineralized insects of the Crato *Lagerstätte*.

2. Geological background

The Araripe Basin is an intracratonic basin located in northeastern Brazil, situated in the central part of Borborema province. The basement of this region consists of Precambrian gneiss and migmatite terrains, which were affected by extensive rifting processes resulting from the split between Africa and South America during the break-up of Pangaea (Matos, 1992). The Araripe Basin is composed of the Cariri Formation, proposed by Beurlen (1962) (Late Ordovician/Early Devonian). There are four further supersequences (Assine *et al.* 2014): (1) the Pre-rift Supersequence: siliciclastic fluvial-lacustrine sediments from both the Brejo Santo and Missão Velha formations (Late Jurassic); (2) the Rift Supersequence: deltaic, fluvial and lacustrine siliciclastic sediments from the Abaiara Formation (Early Cretaceous); (3) the Post-rift I Supersequence: siliciclastic fluvial-lacustrine sediments from the Barbalha (pelites and sandstones), Crato (pelites and carbonates), Ipubi (evaporites) and Romualdo (carbonate concretions) formations, these units occurring within the Santana Group (Aptian); (4) the Post-rift II Supersequence: Cenomanian siliciclastic fluvial sediments from both the Araripina and Exu formations. The relief is marked in the landscape by the Chapada do Araripe, a plateau smoothly inclined westwards and surrounded by steep cliffs. The Chapada do Araripe is bordered by plain sedimentary deposits distributed mainly on the east and NE flanks, a region named Vale do Cariri (Fig. 1).

Several lacustrine depositional episodes have been recognized in the Araripe Basin. The second lacustrine episode took place during late Aptian time and led to deposition of fine-grained deltaic sandstone units (Barbalha Formation), which interlink with several carbonate and siliciclastic units in the Crato Formation (Arai & Assine, 2020; Melo *et al.* 2020; Coimbra & Freire, 2021). These lacustrine carbonate facies are predominantly composed of micritic laminated limestones and have a calcite composition with a low magnesium content (Catto *et al.* 2016).

The Crato Formation consists of carbonate layers more than 20 m thick (Assine, 2007), interbedded with siliciclastic sediments. Their origin is attributed to transgressive–regressive events associated with the expansion and contraction of a lacustrine system (Heimhofer *et al.* 2010). The depositional environment of the Crato Formation is interpreted as a restricted lacustrine or lagoon system with a stratified water column. The lake/lagoon bottom was hypersaline and anoxic (Heimhofer *et al.* 2010). Recently, Warren *et al.* (2017) and Varejão *et al.* (2019, 2021) suggested a shallow hypersaline coastal lacustrine system dominated by benthic microbial mats. The Crato Formation is divided into four members including, from bottom to top: the Nova Olinda, Caldas, Jamacaru and Casa de Pedra (Martill *et al.* 2007). The lowest Nova Olinda Member crops out in the northern and eastern flanks of the Araripe Basin, where the fossil insects from this study were found. The palaeoenvironmental conditions and exceptional preservation of fossils have made the Crato Formation well known worldwide as a Cretaceous fossil *Lagerstätte* (Martill *et al.* 2007).

3. Material and methods

3.a. Fossil material

Specimens used in this research are deposited in the scientific palaeontological collection of the Laboratório de Paleontologia

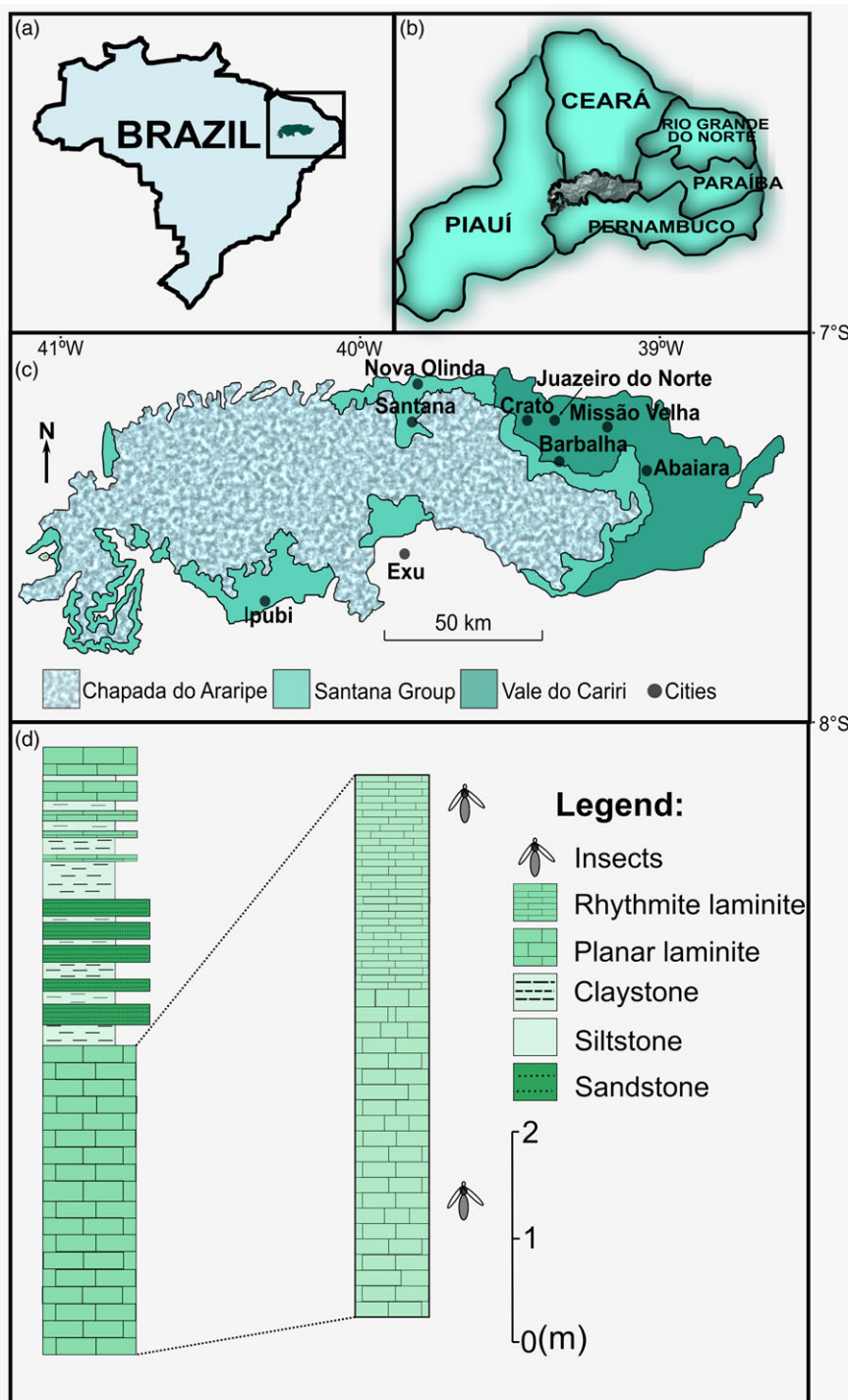


Fig. 1. (Colour online) Location and geological setting of the Crato Lagerstätte. (a) Position of the Araripe Basin in the Brazilian territory. (b) Position of the Araripe Basin in NE Brazil. (c) Toponymic and geological map of the Araripe Basin Crato Formation outcrops associated with the Santana Group. (d) Stratigraphic scheme of the Crato Formation highlighting the Nova Olinda Member, recognized as the Crato Lagerstätte.

of the Universidade Federal do Ceará (Brazil). In all, 138 mineralized insects recovered from the Nova Olinda Member were studied for this analysis (online Supplementary Material Table S1). The main analysis, at hand scale, was performed on mineralized specimens preserved in pale-yellow limestone slabs. At this stage, we observed the degree of completeness, articulation and compaction of each mineralized insect. The microscopic and spectroscopic results presented here are from the analyses of the following samples: LP/UFC CRT 122, LP/UFC CRT 708, LP/UFC CRT 720, LP/UFC CRT 1156, LP/UFC CRT 1822, LP/UFC CRT 1834, LP/UFC CRT 1896, LP/UFC CRT 2055, LP/UFC CRT 2083, LP/UFC CRT

2204, LP/UFC CRT 2388, LP/UFC CRT 2529 and LP/UFC CRT 2647.

3.b. Scanning electron microscopy and large-field energy dispersive spectroscopy

The scanning electron microscopy and energy dispersive X-ray spectroscopy (SEM-EDS) analyses were performed in the Central Analítica at the Universidade Federal do Ceará (UFC). Micromorphological measurements of the fossil insects were conducted by SEM in a Quanta-450 electron microscope (FEI) with a

field-emission gun (FEG) equipped with a gaseous analytical detector (GAD), coupled to an X-ray detector (model 150, Oxford) for EDS. Specimens were prepared by mounting on aluminium stubs with a black carbon cement. The fossil insects were then inserted into the microscope chamber without other previous preparation. The micrographs were obtained using a working distance of 10 mm. Analyses were performed in a low vacuum to avoid sample charging. Images were acquired at a beam acceleration voltage of 20 kV, using a resolution of 1024 × 884 pixels per image. The images were processed and exported on AZtec software (version 3.0/Oxford).

3.c. Fourier transform infrared and Raman spectroscopy

The spectroscopic analyses were performed in the Laboratório de Espectroscopia Vibracional e Microscopia (LEVM), Departamento de Física, at the UFC. The Raman spectra were obtained with a LabRAM HR (Horiba) spectrometer equipped with a liquid N₂-cooled CCD detector behind a 600 g/mm grating. Acceptable spectra were measured using 785 nm laser radiation for excitation (~2 mW at the sample surface). The laser power was set to ~1 mW on the samples. In this investigation, the Fourier transform infrared (FTIR) spectra were measured directly by using a Vertex 70 (Bruker). FTIR data were collected in the spectral range from 200 to 4000 cm⁻¹. No sample preparation was necessary. The Raman and FTIR spectra were analysed in the software Origin 9.2.

4. Results

4.a. Morphological details at hand-specimen scale

Crato mineralized insects typically appear as orange-brown to dark-brown specimens preserved in pale-yellow to reddish limestone slabs. This type of preservation consists of iron (III) oxide hydroxy replacements of former sulfide minerals that replicated the original cuticle. Crato Formation insects displaying this type of preservation are often uncompact, articulated and are complete with antennae, head, thorax, abdomen, legs, articulated wings and other appendages (Fig. 2a–c). These specimens also reveal details of the wings or elytra, often displaying a well-defined venation pattern. Abdomens retain structures such as cerci, caudal gills, ovipositors and legs, which are often well articulated with spines, setae and spurs. These sets of structures are significant in taxonomic phylogenetic analyses, and are employed to estimate the historical relationships among the different insect taxa.

Exceptionally, many disarticulated oxide-hydroxide insects, preserved as fragmentary remains or isolated body segments, still retain remarkable morphological details. This suggests that damage to these insects was probably caused by biotratonic processes prior to burial. However, many of the Crato mineralized insects appear poorly preserved in hand specimens, and closer examination shows that the damage has been caused by diagenetic alteration rather than the result of biotratonic processes (*in vivo* or post-mortem decay). These diagenetic altered insects can appear complete but reveal little to no morphological detail (e.g. ommatidia, wing veins and spines). This style of alteration makes a high classification uncertain even at the order, suborder or family level. In particular, these poorly preserved specimens can be easily damaged by touching, and are commonly encountered in the weathered pale-yellow limestones. After thorough investigations, we have found three types of alterations in Crato insects. The most common type involves insects with iron-oxide overgrowths that reduce morphological fidelity (Fig. 2d–f). This distinctive feature

provides a rust-like hue to insects. The specimen can be fully articulated but possesses a body obscured by iron-oxide overgrowth (e.g. head or thorax). Here, the loss of palaeontological information is usually partial. Secondly, weathered insects appear with light-grey to black coatings. These later coatings can overlap diagnostic features such as wing veins, head appendages or even entire body parts. In particular, this feature gives a ‘dirty’ appearance to fossil insects and is often associated with dendrites. Insects exhibiting this type of alteration also have a rusty appearance (Fig. 2g, i, j). The third type of alteration corresponds to the insects recorded only by their imprint left on the limestone. These fossils are found as two-dimensional imprints of insects or of their parts (Fig. 2h, k, l). Fossil imprints can record information about the external shape of organisms but without complete details or delicate appendages. Owing to the lack of details of the original cuticle, a faithful taxonomic description is hampered. Overall, this type of alteration process results in ‘depleted’ versions of the specimens, where telodiagenetic fluids dissolve away the mineral replacements leaving behind only the external outlines of former insects.

4.b. Scanning electron micrograph analysis

The SEM analysis revealed that preservation of the Crato Formation insects includes individual cuticular surface structures (Fig. 3). Overall, the cuticle surface retains fine morphological details, built by sub-spherical to spherical grains with diameters mainly in the range of 5–15 μm. These structures are commonly arranged as globular aggregates or as close-packing grains. The micrographs also revealed anhedral to euhedral crystals of variable sizes and organization, and many of the grains observed in these fossils were shown to be hollow. This suggests that these crystals may be classified as pseudoframboids (Berner, 1970; Kribek, 1975; Ohfuji & Rickard, 2005) of a mineral precursor. For further clarification of the mineral fabrics of Crato insects, see Barling *et al.* (2020). These crystal structures have not been observed within extant insect cuticle and do not appear to be of a biological origin; they are often interpreted as mineral fabrics produced during the early diagenesis.

In the best articulated specimens at hand scale, the high magnification revealed that the cuticle can also be replaced by a polygonal lamellar arrangement, with grains of ~1 μm in diameter (Fig. 3a). In these insects, any loss of preservation fidelity is partial or occurs locally on a micron scale (Fig. 3b, c). The cuticle is preserved as a massive film without microtextural differentiation and commonly with sensilla insertion holes in the surface (Fig. 3d). This cuticular arrangement suggests a direct replacement of insect tissue.

The higher magnification investigation of the insects not well preserved at hand scale shows different textural characteristics at the micro scale. Crato Formation insects preserved as two-dimensional imprints commonly record details of the original external form. In micrographs, they display clusters of cryptocrystals or isolated pseudomorphs associated with calcite crystals (Fig. 3e). Fossil cuticles are preserved by a thin discontinuous layer. It is sometimes difficult to distinguish the boundaries between the fossil and carbonate matrix.

The presence of microcracks in the insect cuticles of the Crato Formation has been frequently reported (Delgado *et al.* 2014; Barling *et al.* 2015, 2020; Osés *et al.* 2016; Bezerra *et al.* 2020, 2021; Dias & Carvalho, 2020, 2021; Prado *et al.* 2021). Crato insects with iron-oxide overgrowths show intricate zones of microcracks associated with compact cuticular surfaces without individualized



Fig. 2. (Colour online) Examples of mineralized/impression insects from the Crato Formation in different types of preservation. (a–c) Crato insects well preserved at hand scale: Coleoptera (LP/UFC CRT 2529), Caelifera (LP/UFC CRT 2083) and Hymenoptera (LP/UFC CRT 2768), respectively. (d–f) Examples of insects with iron-oxide overgrowths: Ensifera (LP/UFC CRT 1834), Heteroptera (LP/UFC CRT 708) and Odonata (LP/UFC CRT 1152), respectively. (g, i, j) Mineralized insects with black coatings sometimes associated with dendrites: Ensifera (LP/UFC CRT 2388), Odonata (LP/UFC CRT 1156) and Ensifera (LP/UFC CRT 2647), respectively. (h, k, l) Crato insects preserved as imprints: Phasmatodea (LP/UFC CRT 2698), Isoptera (LP/UFC CRT 1896) and Caelifera (LP/UFC CRT 2204), respectively. Scale bars = 10 mm.

crystals (Fig. 3f). The microcracks commonly appear in isolation but they can also link up, demonstrating that this type of damage has the potential to be quite extensive. They are connected to each other by straight contacts in a perpendicular way, but curved microcracks have also been observed. These microcracks are commonly empty, and rarely filled with minerals. Crato

insects with black coatings show regions of the cuticle replaced by inequidimensional, spherical to sub-spherical microcrystals forming alveolar aggregates with partially corroded surfaces, but sometimes areas without individualized crystals can also occur. Such evidence reveals the intense oxidation of these mineralized replacements.

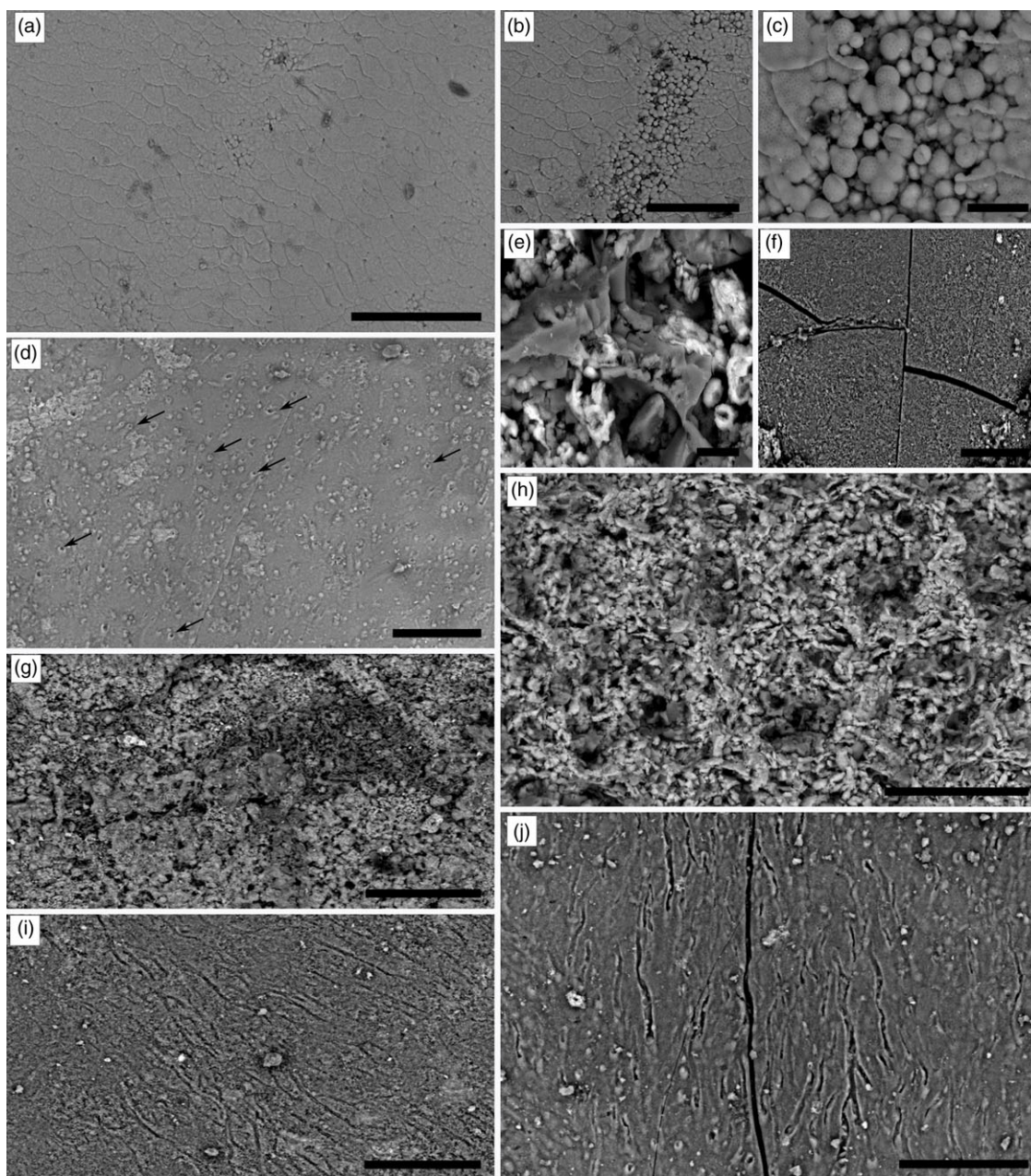


Fig. 3. (Colour online) Scanning electron micrograph analysis for cuticular characterization of Crato Formation insects. (a) Cockroach (LP/UFC CRT 2055) showing cuticular high fidelity; scale bar = 100 μm . (b) Local loss of cuticle fidelity in (a); scale bar = 50 μm . (c) Detail of the microtexture depicted in (b); scale bar = 10 μm . (d) Beetle (LP/UFC CRT 2529) epicuticle with sensilla insertion holes (indicated by arrows) on its surface; scale bar = 50 μm . (e) Caelifera (LP/UFC CRT 2204) preserved as two-dimensional imprints with inequidimensional and spherical to sub-spherical micro-cryptocrystals of iron oxides associated with crystals of calcite; scale bar = 10 μm . (f) Surface micro-cracking of a cricket epicuticle (LP/UFC CRT 1834) with iron-oxide overgrowths; scale bar = 50 μm . (g) Cricket (LP/UFC CRT 2388) with black coatings showing microfabric formed by sub-spherical loosely packed grains; scale bar = 100 μm . (h) Ommatidia of a Heteroptera (LP/UFC CRT 708) with iron-oxide overgrowths showing pseudoframboids and alveolar aggregates of iron-oxide crystals associated with dissolution cavities; scale bars = 50 μm . (i) Heteroptera (LP/UFC CRT 720) epicuticle with iron-oxide overgrowths scratched by sets of grooves generated by oxidation reactions; scale bar = 50 μm . (j) Detail of the Heteroptera (LP/UFC CRT 720) epicuticle showing grooves associated with microcracks; scale bar = 50 μm .

Both styles of preservation, associated with black coatings and with iron-oxide overgrowths displaying aggregates of micro-cryptocrystals, replace the external cuticle, with the corroded surfaces and empty cavities previously occupied by crystals (Fig. 3g, h). Specimens with iron-oxide overgrowths also show a locally rugged and pitted surface scratched by sets of grooves (Fig. 3i). The grooves retain a flow aspect and sometimes appear associated with microcracks (Fig. 3j).

4.c. Raman and FTIR spectroscopy analyses

Raman spectra of Crato Formation insects are recorded mainly in the spectral range 160–710 cm^{-1} with single peaks between 1280 and 1320 cm^{-1} (online Supplementary Material Table S2). Figure 4a shows the Raman spectra profile obtained from an insect preserved as a two-dimensional imprint with bands at 229, 297, 413, 684 and 1319 cm^{-1} . The bands at 229, 297 and 413 cm^{-1} are attributed to Fe–O symmetry stretching, Fe–OH symmetry

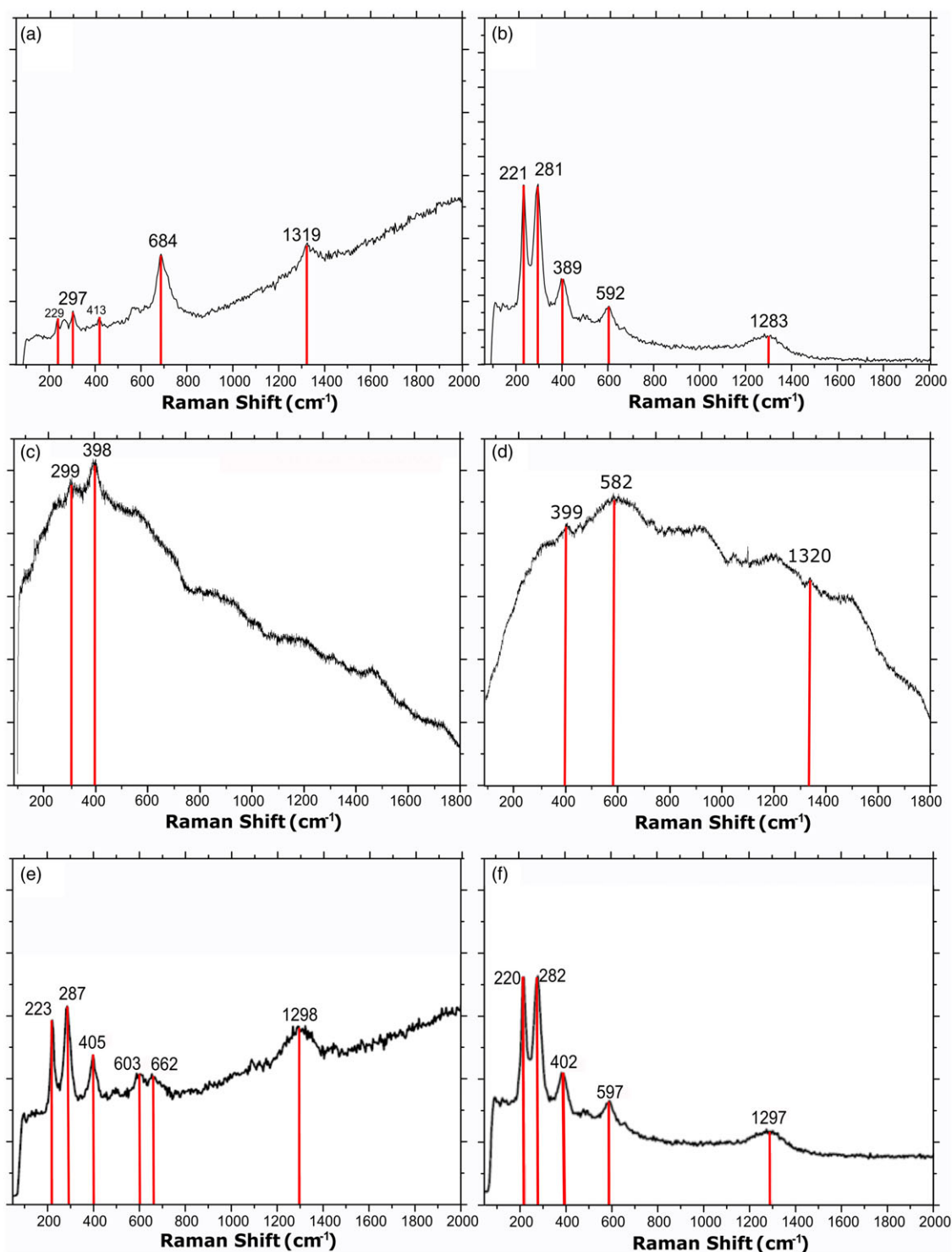


Fig. 4. (Colour online) Raman spectra of insect cuticles of (a) Caelifera (LP/UFC CRT 2204) preserved as two-dimensional imprints, (b) Odonata (LP/UFC CRT 1156) associated with dendrites and (c, d) spectra of crickets with iron-oxide overgrowths, LP/UFC CRT 122 and LP/UFC CRT 1822, respectively. (e, f) Raman spectra of mineralized insects that retain fine details of morphology at hand scale: Blattodea (LP/UFC CRT 2055) and Caelifera (LP/UFC CRT 2083), respectively.

bending and Fe–O symmetry bending, respectively (Das & Hendry, 2011; Mohapatra *et al.* 2011). The intense band at 684 cm⁻¹ is attributed to Fe–O symmetric stretching vibration, which is often associated with α-FeOOH (de Faria & Lopes, 2007). The weak peak at 1319 cm⁻¹ is characteristic of various iron-oxide and iron-hydroxide minerals (Marshall & Marshall,

2013). Figure 3b shows the Raman spectra obtained from a Crato insect with black coatings bearing two intense bands at 221 cm⁻¹ and 281 cm⁻¹ attributed to Fe–O symmetry stretching and Fe–O bending, respectively (Legodi & de Waal, 2007). The broad band centred at 1283 cm⁻¹ is often assigned to iron oxides (Hassan *et al.* 2010). The presence of iron oxides is reinforced by

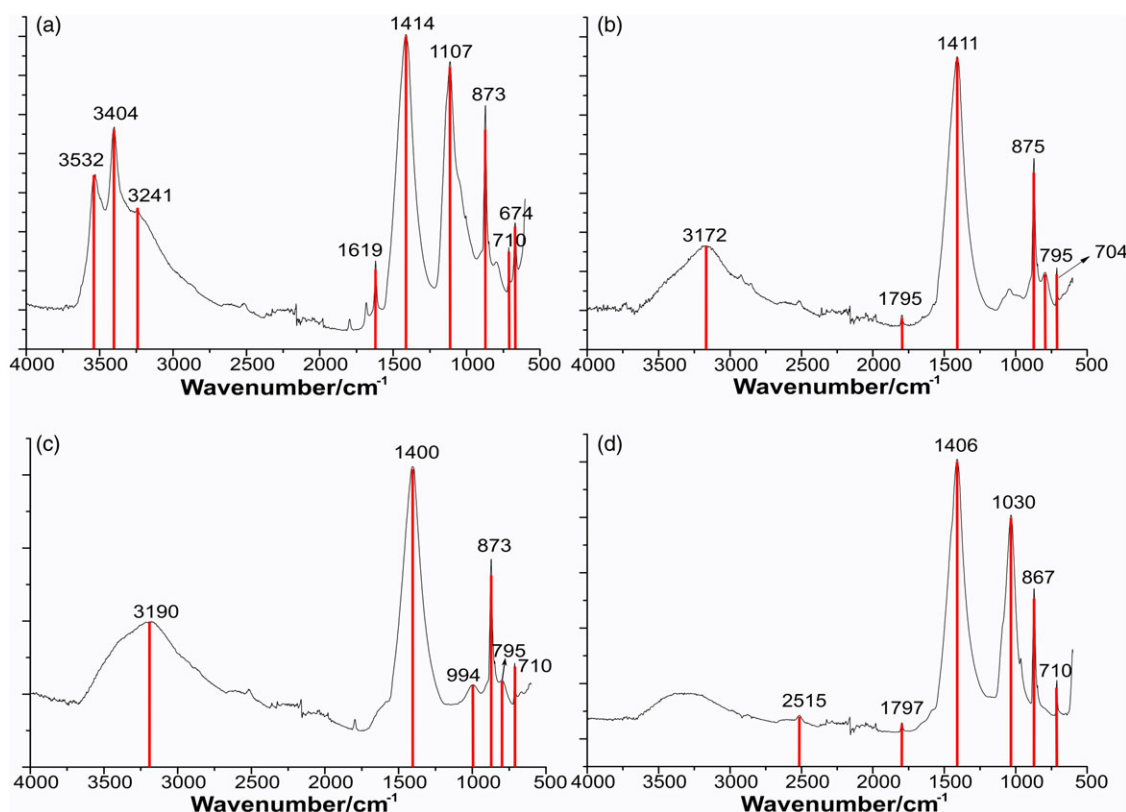


Fig. 5. (Colour online) Infrared spectra of Crato insects. (a) Isoptera (LP/UFC CRT 1896) preserved as two-dimensional imprints, (b) a cricket (LP/UFC CRT 834) with iron-oxide overgrowths, (c) a cricket (LP/UFC CRT 2647) with black coatings and (d) a Heteroptera (LP/UFC CRT 720) well preserved at hand scale.

the band at 389 cm^{-1} , the vibration of Fe–OH (Li & Hihara, 2015). The band at 592 cm^{-1} attributed to Mn–O stretching mode is taken as characteristic for $\alpha\text{-Mn}_2\text{O}_3$ (Julien *et al.* 2004). This band indicates that iron compounds are found in close association with manganese oxide minerals.

Notably, the Raman spectra obtained from Crato insects with iron-oxide overgrowths display a high background noise (Fig. 4c, d). A possible explanation for this background is the presence of an OH group generating interference. The Raman spectra were also affected by fluorescence artefacts, and the broad bands may reflect the low degree of crystallinity of the fossil material. Regardless, the Raman spectra of the insects with iron-oxide overgrowths show bands associated with the mineral goethite (Zuo *et al.* 2003). In Raman spectra of insects that retain fine morphological details, bands attributed to haematite can be observed (Fig. 4e, f). The presence of haematite is marked by bands at 220, 287, 402 and 603 cm^{-1} (Legodi & de Waal, 2007).

The FTIR spectra of insects show heterogeneity, with different peaks recorded at various positions. FTIR signals were observed mainly in two spectral regions: $600\text{--}1000\text{ cm}^{-1}$ and $3200\text{--}3600\text{ cm}^{-1}$ (online Supplementary Material Table S2). The graphics exhibit a spectral region where it is possible to observe bands related to OH-stretching vibrations. The spectrum of a Crato insect preserved as a two-dimensional imprint show bands at 674, 710, 873, 1107, 1414, 1619, 3241, 3404 and 3532 cm^{-1} (Fig. 5a). The band at 674 cm^{-1} is usually attributed to lattice absorption of iron-oxide (Tiwaria *et al.* 2015). The band at 710 cm^{-1} appears associated with bands at 873 cm^{-1} and 1414 cm^{-1} , which suggests characteristic bands of calcite (Rodríguez-Blanco *et al.* 2011). The peak at 1107 cm^{-1} can be assigned to the symmetric stretching mode of CaO (Gunasekaran

& Anbalagan, 2007). The weak band at 1619 cm^{-1} can be attributed to O–H bending vibration (Raji *et al.* 2020). Significant bands around 3241, 3404 and 3532 cm^{-1} are assigned to the OH-stretching vibrations of the hydroxyl units $\nu(\text{OH})$ (Frost *et al.* 2011, 2016; Frost & Xi, 2012). These bands show that this sample experienced chemical transformations under extremely wet conditions. The FTIR spectrum (Fig. 5b) of an insect with iron-oxide overgrowths shows a wide band centred at 3172 cm^{-1} in the region related to OH-stretching vibrations. This remarkable wavenumber region probably consists of the overlapping of two or more components in the range $3270\text{--}3180\text{ cm}^{-1}$. Bands at 1411 and 1795 cm^{-1} correspond to stretching of CO_3^{2-} . The band at 795 cm^{-1} can be assigned to Fe–O–H bending vibrations commonly associated with $\alpha\text{-FeOOH}$ (Musić *et al.* 2003). Figure 5c shows the FTIR spectrum obtained from a Crato insect with black coatings. The broad band at 3190 cm^{-1} can be attributed to O–H stretching vibration. The bands at 710, 873 and 1400 cm^{-1} are assigned to the antisymmetric stretching modes of calcium carbonate (Frost *et al.* 2008). The band at 994 cm^{-1} can be tentatively assigned to Fe–O vibrations. This band is often obscured in goethite. The FTIR spectrum (Fig. 5d) of a well-preserved insect at hand scale also exhibits the characteristic peaks of calcite. However, the wavenumber region between 3000 and 3600 cm^{-1} appears less prominent here. In addition, the band around 1030 cm^{-1} is caused by the vibration of crystalline Fe–O mode, which is characteristic of haematite (Pal & Sharon, 2000).

4.d. Energy dispersive X-ray spectroscopy

Elemental analyses revealed that iron is more concentrated in fossil cuticles than in the carbonate matrix, while calcium is the opposite. The distribution of oxygen is in accordance with the presence of

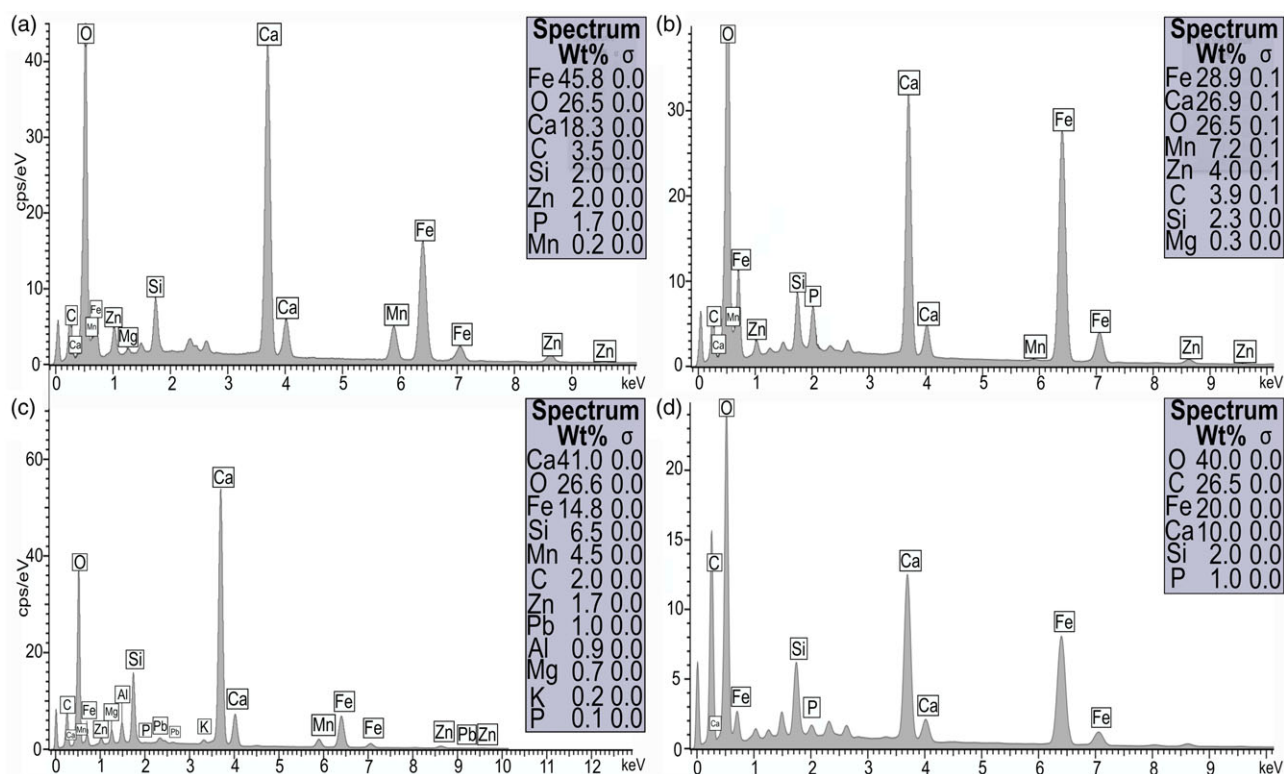


Fig. 6. (Colour online) Energy dispersive X-ray spectroscopy point spectra of (a) rust-like Heteroptera (LP/UFC CRT 708) with iron-oxide overgrowths, (b) a cricket (LP/UFC CRT 2388) with black coatings, (c) Caelifera (LP/UFC CRT 2204) preserved as two-dimensional imprints and (d) a mineralized cockroach (LP/UFC CRT 2055) fully articulated and well preserved.

iron compounds replacing the fossils and the carbonate composition of the rock matrix. The insects with iron-oxide overgrowths contain a higher abundance (wt %) of iron than the other specimens (Figs 6a, 7a). In the spectrum of these insects, silicon, carbon, zinc, manganese and phosphorus are also represented. On the other hand, Crato insects with black coatings display a higher abundance (wt %) of manganese (Figs 6b, 7b). The ‘depleted’ insects preserved as imprints of outer cuticle exhibit a wide range of elements with a predominance of calcium (Figs 6c, 7c). Aluminium, lead, magnesium, potassium, silicon and manganese are also reported (Fig. 6c). Fully articulated insects with fine morphological details display a higher abundance of carbon and a lower abundance of calcium (Fig. 6d), and the conspicuous presence of phosphorus has also been documented (Fig. 7d). Overall, EDS data support that the fossil cuticles have high concentrations of iron and oxygen, suggesting that original pyrite has been replaced by iron oxides/hydroxides due to post-diagenetic events (Fig. 7).

5. Discussion

5.a. Micro-structure preservation of weathered insects from the Crato Formation

The spectroscopic results revealed that the fossil insects studied here are preserved by iron-oxide/oxyhydroxide compounds, mainly haematite and goethite. Overall, SEM analysis showed that insect cuticles are preserved by globular aggregates or close-packing grains. Mineralized specimens exhibiting more morphological details at hand scale (best preserved) show cuticle surfaces with a polygonal lamellar arrangement and grains of ~1 µm in diameter.

These insects display microtextural surfaces with little differentiation. The loss of fidelity is only partial and sometimes still maintains sensilla insertion holes. On the other hand, our results also show that Crato mineralized insects poorly preserved at the hand scale level show different textural characteristics at the micro scale. These insects commonly display cuticle details preserved by sub-spherical to spherical crystals in variable organizations with diameters mainly in the range of 5–15 µm. These characteristics are clear evidence of intense weathering experienced by Crato mineralized insects. Macroscopically, we highlighted at least three types of post-diagenetic alterations with the potential to distort morphological information essential for systematic studies. The alterations can be observed in specimens with iron-oxide overgrowths, insects with black coatings sometimes associated with dendrites and those preserved as two-dimensional imprints. Microscopically, Crato insects with iron-oxide overgrowths and black coatings are dominated by one fabric arranged into spherical or cylindrical aggregates sometimes possessing needle-like grains and hollow crystals. They also display microcracks and crystal aggregates associated with an alveolar habit, partially corroded surfaces and empty structures of dissolution cavities. In micrographs of insects with iron-oxide overgrowths, flow structures represented by sets of micro-grooves often appear as a striking feature. These scratches are likely the result of intense surface dissolution. The insects preserved as imprints retain discontinuous clusters of cryptocrystals or isolated aggregates, evidence of an intense oxidation process. Intrastratal fluids leach away the insect mineral replica, leaving only parts of the body behind. Undoubtedly, Crato insect imprints represent the most intense type of alteration, and individuals showing this condition are rarely recovered for taxonomic purposes.

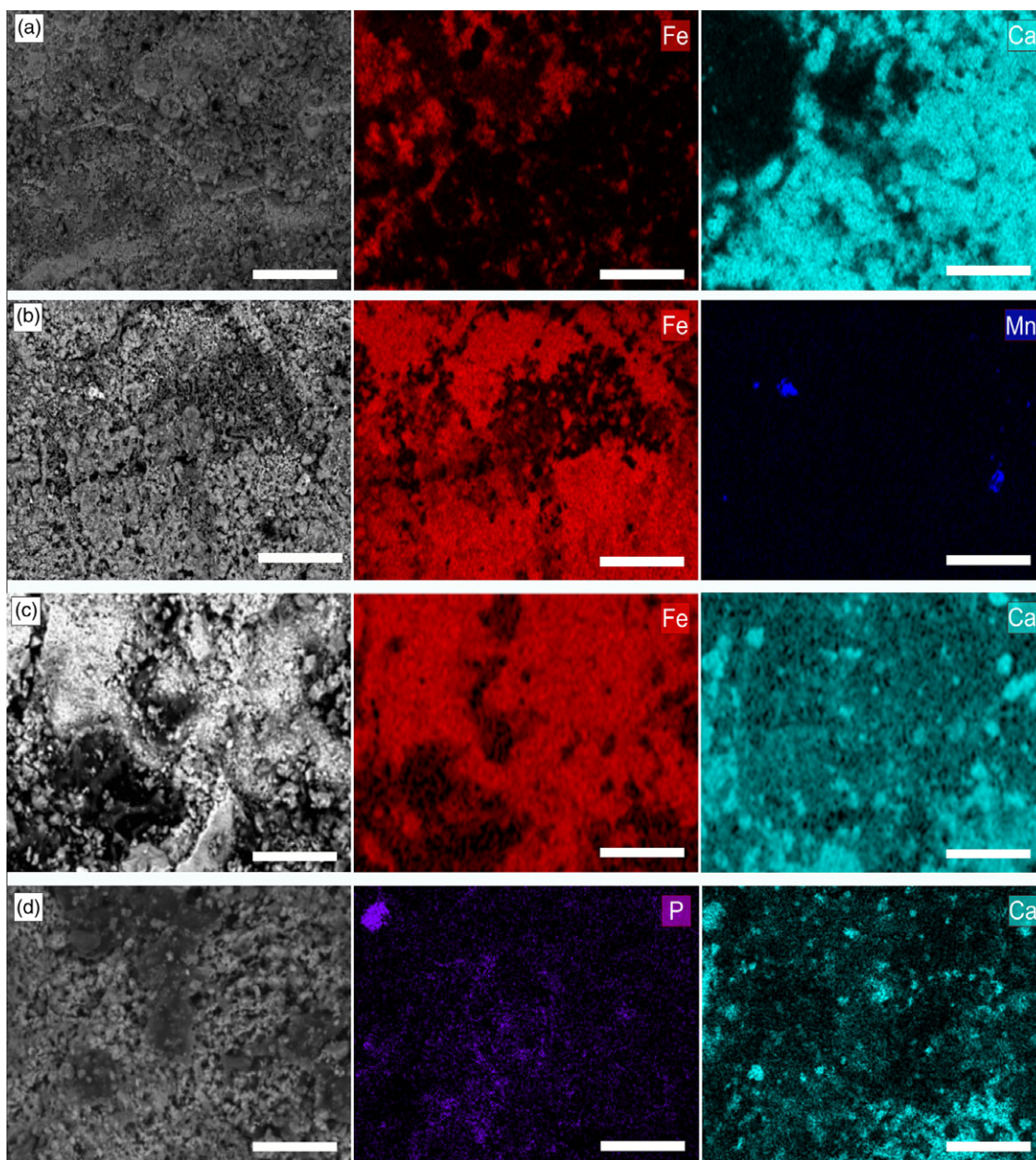


Fig. 7. (Colour online) Energy dispersive X-ray spectroscopy elemental map of Crato insects. (a) Secondary electron micrograph of Heteroptera (LP/UFC CRT 708) with iron-oxide overgrowths and the elemental maps of iron and calcium; scale bars = 50 μm . (b) Micrograph of a cricket (LP/UFC CRT 2388) with black coatings and the elemental maps of iron and manganese; scale bars = 50 μm . (c) Micrograph of a Caelifera (LP/UFC CRT 2204) preserved as two-dimensional imprints and the elemental maps of iron and calcium; scale bars = 100 μm . (d) Secondary electron micrograph of a well preserved cockroach (LP/UFC CRT 2055) and the elemental maps of phosphorus and calcium; scale bars = 50 μm .

Our secondary electron analysis shows that Crato mineralized insects are preserved in a variety of mineral styles. They are interpreted as mineral fabrics produced during the early diagenesis that replicated fine details of the cuticle and other soft tissues. The Fe-oxide/hydroxide pseudomorphs are similar to precursor pyrite. The formation of pyrite replacements and their direct involvement in the replication of insect morphology are intrinsically associated with the time the fossils spent in the bacterial sulfate reduction zone of the sediment (Schiffbauer *et al.* 2014). The taphonomic pathways of pyritized insects during the early diagenesis of the Crato Formation have been well documented in previous studies (Barling *et al.* 2015, 2020; Osés *et al.* 2016; Bezerra *et al.* 2020; Dias & Carvalho, 2020, 2021).

Nonetheless, the scattered distribution of the aggregate particles and the variety of their arrangements indicates a complex oxidation process with several probable stages. Dissolution cavities, microcracks, flow structures and hollow crystals with corroded surfaces merged into larger aggregates are microtextural features that evidence chemical weathering under variable water conditions.

5.b. Transformation of Fe-oxide/hydroxide pseudomorphs

Pyrite oxidation is a complicated process that includes several types of oxidation–reduction reactions, hydrolyses and complex ion formation. The transformation of pyrite in an oxygen-containing

environment may proceed by different mechanisms under different conditions. Parameters such as temperature, oxygen concentration and flow conditions can all affect the transformation process (Jorgensen & Moyle, 1982). Oxidation is a major process in the dissolution of pyrites, and aqueous oxidation plays a significant role in the production of sulfuric acids as a result of natural weathering of pyritic rocks and shale (Rimstidt & Vaughan, 2003). Overall, ferrihydrite is produced as an intermediate phase between the primary sulfide and the final oxides/hydroxides during the oxidation of pyrite in an aqueous environment (Nordstrom, 1982). Ferrihydrite is metastable under oxic conditions, gradually converting to the more crystalline and stable goethite and haematite (Cudennec & Lecerf, 2006). Ferrihydrite dissolves to neutral pH (7–8) and transforms to haematite. In contrast, goethite formation occurs under either acidic or alkaline conditions (Das *et al.* 2011). The preservational textures observed in the cuticle of mineralized insects from the Crato Formation consist primarily of pyrite framboids and pseudoframboids (Barling *et al.* 2015; Osés *et al.* 2016; Bezerra *et al.* 2020). These microtextural characteristics indicate that the mineral fabrics of insects are very similar both after and before post-diagenetic changes. In this case, the hypothesis of transformation of pyrite through the dissolution–crystallization process is unlikely. Therefore, the transformation of pyrite into goethite and haematite most likely occurred in the solid state.

The oxidation of pseudoframboidal pyrite is considered to be fast owing to its high specific surface area (Pugh *et al.* 1984). However, the formulation of a consistent oxidation reaction of the pyrite surface is not sufficiently characterized, and oxidation of pseudoframboid surfaces may occur upon contact with meteoric water and the Earth's oxygenic atmosphere, where O_2 and Fe^{3+} play a key role. Initially, transformation involves the adsorption of O_2 and water to the pyrite surface. Singer & Stumm (1970) suggested that Fe^{3+} is the major oxidant of pyrite whereas O_2 becomes the predominant oxidant at circumneutral pH. Fe^{3+} is also oxidizing at circumneutral pH, but the reaction cannot be sustained without the presence of dissolved O_2 to perpetuate the oxidation to Fe^{3+} (Evangelou & Zhang, 1994). Schaufuß *et al.* (1998a) found Fe^{3+} oxyhydroxide to be the main product after sulfate during the oxidation process. Jerz & Rimstidt (2004) reported that the FeS_2 oxidation reaction rate decreases with time, and linked the reduced reaction rate to the development of a thin layer of iron on the pyrite surface. The authors proposed that this layer retards oxygen transport and hence induces a possible change from reaction rate. Eggleston *et al.* (1996) hypothesized an oxidation mechanism involving surface cycling of Fe^{2+} and Fe^{3+} , where Fe^{3+} hydroxide or oxide products serve as a conduit for electron transfer from the pyrite surface to molecular oxygen. This involves the transfer of electrons from pyrite Fe^{2+} to oxide Fe^{3+} , and this process takes place preferentially from pyrite Fe^{2+} adjacent to the oxide. Schaufuß *et al.* (1998a,b) also provided a similar explanation for the initial formation of iron oxides on pyrite surfaces. The surface crystal attached to the Fe^{3+} site causes electron transfer from the Fe^{2+} adjacent to the attached O_2 . Then, the second Fe^{3+} adjacent to the first induces Fe^{3+} oxide propagation, resulting in the formation of $FeOOH$, which can be dehydrated to Fe_2O_3 later. Gu *et al.* (2020) postulated that pyrite oxidation is limited by diffusion of oxygen at the grain scale, which is in turn regulated by fracturing at the clast scale. Thus, the pyrite oxidative transformation progresses inwards from fractures when observed at the clast scale. Oxidized pyrites often have an oxidation shell and an unoxidized core. Du *et al.* (2021) noted that the degree of pyrite oxidation is relative to the thickness of the oxidation shell. Therefore, the thickness of the

oxidation shell indicates a more oxidizing environment or a longer duration of oxidation. This could be a possible explanation for the numerous hollow crystals observed in the cuticular replicas of Crato insects (Fig. 3e, g, h). Non-oxidized pseudoframboidal crystals would be more vulnerable to erosion. Thus, the hollow crystals observed here could represent a shorter oxidation duration or lower oxygen fugacity.

5.c. Weathering of Crato pyritized insects

Chemical weathering of sedimentary rocks normally produces successions of minerals in different hydration states. Overall, weathered profiles contain several sequences of hydrated–dehydrated–hydrated minerals distributed in zones above and within the ground water table (Chigira & Oyama, 1990). An essential mineralogical change in weathered profiles is the formation of oxides and hydroxides, where goethite and haematite are the main hydrated and dehydrated minerals, respectively (Schwertmann, 1988). Hydrated minerals appear at the bottoms of profiles, close to the ground water table, while dehydrated minerals appear preferentially in the intermediate part between two horizons containing more hydrated minerals. This general distribution is mainly explained by seasonal fluctuations of the intrastratal water within the profiles. The weathering of fossil insects from the Crato Formation seems to have been directly influenced by meteoric fluids. The oxidation of framboidal pyrites of cuticles of Crato insects is limited by diffusion of oxygen through the carbonate matrix. The transport of O_2 depends on the penetration of water, which is in turn limited by the formation of fractures and pores. At the landscape scale, the oxidation process is limited by the movement of meteoric fluids into the carbonate matrix. This idea is supported by observations showing cases where pyrite oxidizes to a depth of metres (e.g. 2 to 10 m) in crystalline rocks and pyrite-rich black shales (Wildman *et al.* 2004; Drake *et al.* 2009).

Although efforts to delimit the stratigraphic position of the different fossil groups in the Crato Formation are rare in the literature, mineralized insects seem to be restricted to the uppermost part of the interval II proposed by Varejão *et al.* (2019). This interval consists of yellow to red-coloured laminites with domal stromatolites and halite hoppers (Varejão *et al.* 2019). According to these authors, these layers are more fossiliferous in the Nova Olinda region, where they crop out on quarry fronts. Recently, Corecco *et al.* (2022) reported an interval informally named by quarry workers as 'veio do besouro', from which most Crato mineralized insects are recovered. This interval corresponds to the uppermost part of the Nova Olinda Member. The non-homogeneous mineral fabrics observed in Crato insect replicas suggest that the transformation of the pyrite was limited by transport of reactants through the matrix to the grain surface. At this scale, the transport of reactants specifically depends on the porosity and permeability of the matrix. The laminated limestone of the Crato Formation shows average porosity and permeability values of 12 % and 0.04 mD (Miranda *et al.* 2016). For most relatively unfractured low-porosity carbonate zones within quarry fronts, reactants move by diffusion (Gu *et al.* 2020). During weathering, iron oxides slowly replace iron sulfide while retaining the external shape. The observation that the oxidation of framboids in Crato insects was accompanied by small changes in volume is consistent with the pseudomorphic nature of the transformation of pyrite to iron oxides (Putnis, 2009).

Although we did not find a characteristic spectroscopic spectrum for each type of post-diagenetic alteration identified here, our data show that insects well preserved at hand scale are

preferentially replaced by haematite. However, Osés *et al.* (2016) and Bezerra *et al.* (2020) have already reported traces of goethite in well-preserved insects from the Crato Formation. Therefore, pyritized insects that retain privileged morphological information can be slowly oxidized to haematite or goethite by diffusion through the carbonate matrix. In this case, goethized insects faithfully replicated at the micro scale are thought to have been oxidized in wetter conditions than the haematized insects. Nonetheless, our spectroscopic results showed that Crato insects with iron-oxide overgrowths are preferentially preserved by goethite (Fig. 8). This secondary goethite seems to correspond to a rehydration process which is thought to be responsible for the destruction of the morphological fidelity acquired in the pyritization stage during early diagenesis. Specimens with black coatings are often associated with dendrites and other fluid structures related to manganese oxides/hydroxides (Figs 4b, 6b). The genetic mechanism for the formation of manganese dendrites and other low-crystallinity products is the invasion of sedimentary discontinuities by mineralized fluids through cracks. The intensification of this process progressively diminishes the morphological fidelity of the fossil insects affected by it. Both types of alteration with iron-oxide overgrowths and black coatings, the most intuitive sources of Mn^{4+} and Fe^{3+} is the circulation of enriched solutions through the discontinuities of the Crato carbonates. In this scenario, cracking events provoke the injection of these solutions, which travel through the sedimentary body forming different oxidized zones. Under such conditions, manganese ions will precipitate as $MnOOH$ and iron ions as $FeOOH$ (Giovanoli, 1980). These pervasive processes can easily distort or even rub out the morphological information recorded in haematized or goethized insects that maintain the preservation fidelity primarily obtained during pyritization. Consequently, insects preserved as imprints represent the exacerbation of this process, where mineralized replicas are leached away (Fig. 8). Thus, textural, mineralogical and chemical features of Crato mineralized insects damaged during telodiagenesis are indicative of intense palaeoweathering events limited by erosion. Miranda *et al.* (2018) identified in the laminated carbonates of the Nova Olinda Member a series of extensional fractures and secondary structures such as horizontal veins, stylolites and vuggy fractures. These structures become conduits for infiltration of meteoric water, favouring an intense dissolution process. In some outcrops of the Nova Olinda Member, fractures are filled with calcite and/or gypsum, indicating an origin related to telodiagenetic processes (Miranda *et al.* 2012, 2018). Therefore, all types of post-diagenetic deformities observed in Crato insects can be directly linked to these discontinuities in the carbonate matrix. According to Miranda *et al.* (2018), these structural breaks were formed owing to the uplift of the Crato Formation and evolved along pre-existing planes of weakness, generating karstic features in the laminites. Marques *et al.* (2014) suggested that the current topography of the region is the result of a major inversion event that occurred in the Araripe Basin during Quaternary time. Thus, porosity can grow through dissolution and fracturing due to the exhumation of the Crato deposits and subsequent erosion. Mineralized insects of the Crato Formation have been slowly oxidized by diffusion of O_2 through a low-porosity matrix. However, this conservative transformation can be obliterated by a late pervasive event.

The slow oxidation of Crato insects must have been essential to maintain the morphological fidelity obtained in the early diagenesis. The transmission of information conceived under anoxic conditions to the modern atmospheric environment greatly favours

the recovery of specimens. This clearly demonstrates that the high-quality preservation of Crato mineralized insects is a combination of early diagenetic induced mineralization and slow weathering rates in the low-porosity matrix. Therefore, all types of alterations presented in this research were caused by late events that affected fossils positioned in the vicinity of fractures or other secondary structures.

6. Conclusions

The exceptional preservation of mineralized insects from the Crato Formation is attributed to geochemical conditions which allowed the pyritization of their cuticles and internal soft tissues during early diagenesis. Our results of imaging and spectroscopy techniques showed that these mineralized insects were pseudomorphed by iron oxides and hydroxides. Mineral pseudomorphism likely materialized during Quaternary time when the last major uplift event in the Araripe Basin took place. This process transformed the original pyrite into haematite and goethite by slow diffusion of O_2 through a fine carbonate matrix. In this case, haematized and goethized insects faithfully replicated, even at the micro scale, the morphological information obtained during the earlier pyritization. On the other hand, our results also showed at least three types of post-diagenetic alterations with the potential to distort, or even destroy, morphological information from Crato insects. Overall, altered insects are not well preserved at the hand scale and also show different textural characteristics at the micro scale. The alterations can be observed in specimens with iron-oxide overgrowths, insects preserved as two-dimensional imprints and those with black coatings sometimes associated with dendrites. Crato insects with iron-oxide overgrowths are preferentially pseudomorphed by goethite and exhibit characteristic grooves and scratches on the surface of their cuticle at the micro scale. This type of alteration seems to correspond to a rehydration process, which is thought to be responsible for the destruction of the morphological fidelity acquired during the pyritization stage. Individuals with black coatings are often associated with dendrites and other low-crystallinity products related to manganese oxides/hydroxides that overlap primary preservation at the macro and micro scales. Lastly, insects preserved as imprints retain only parts of the cuticle with discontinuous clusters of cryptocrystals or isolated aggregates. This last type represents the most intense weathering experienced by Crato insects, which is when mineralized replicas are leached away.

In summary, we list three major geochemical steps involved in the taphonomic history of mineralized insects from the Crato fossil *Lagerstätte*, excluding biostratinomic processes. Firstly, early diagenetic pyritization of cuticle and labile tissues under hypersaline lacustrine system conditions associated with microbial activity (Catto *et al.* 2016; Varejão *et al.* 2019). This step yielded three-dimensional replicas of insects. Secondly, the transition of palaeontological information obtained under anoxic conditions to an oxic and stable environment. This transformation was provided by slow oxidation *in situ*, keeping morphological details of delicate features, which can shed light on taxonomy and systematics. Thirdly, the pervasive weathering experienced by oxidized insects near fractures or other secondary structures, where reprecipitation and chemical dissolution is intense. This step obscures the palaeontological information partially or entirely; therefore, Crato insects involved in this step are less likely to be recovered for taxonomic studies.

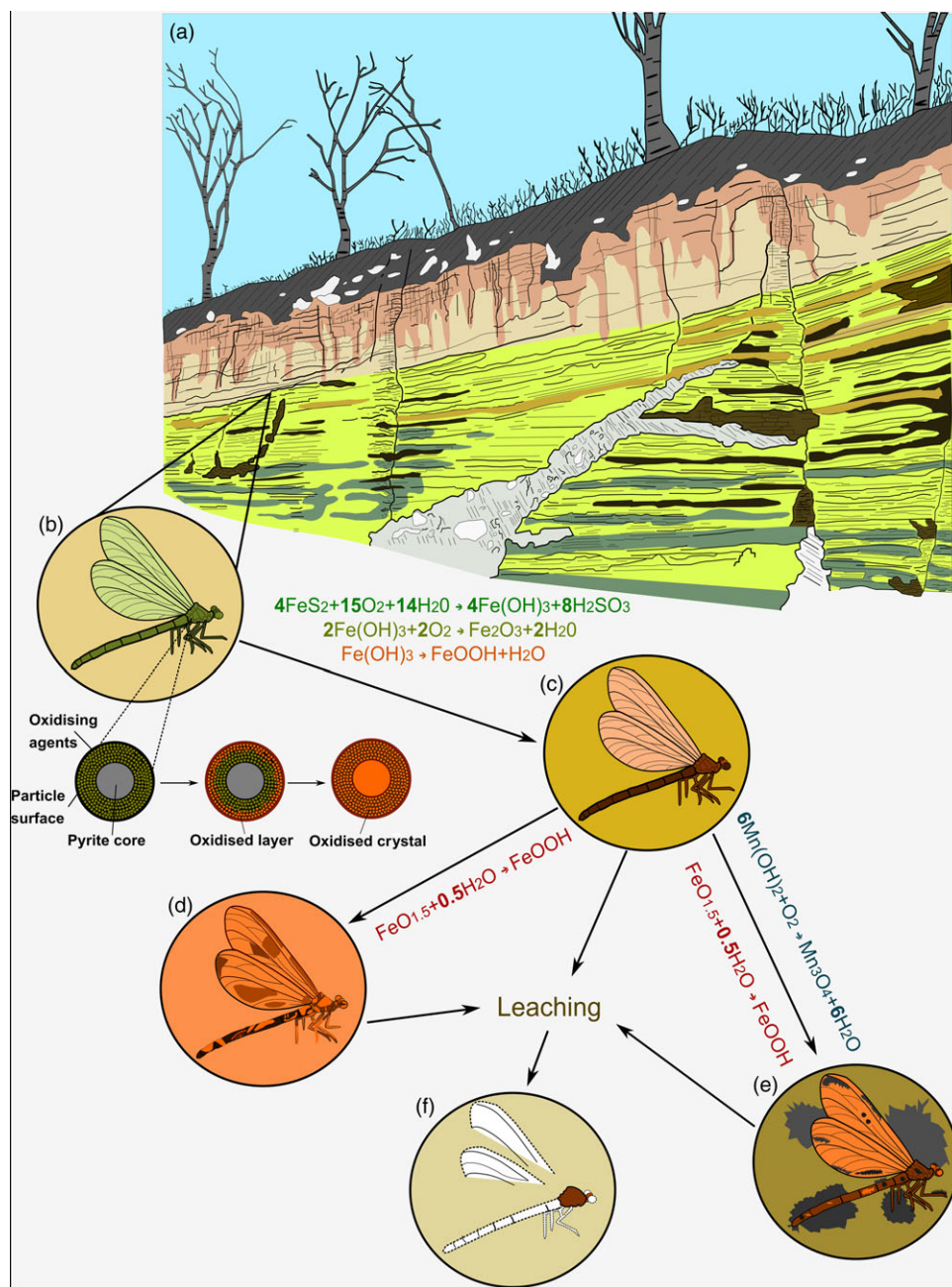


Fig. 8. (Colour online) Hypothetical model for the different weathering pathways of mineralized insects in the Crato Formation after earlier pyritization. (a) Schematic outcrop (quarry front) of laminated limestone from the Nova Olinda Member. (b) Illustration of a pyritized insect where pseudoframboids are transformed into haematite or goethite through the Quaternary by contact with oxidizing agents from the atmosphere. (c) Haematized or goethized insect that retains the fine morphological details acquired during earlier pyritization. (d) Rehydrated insects with iron-oxide overgrowths preserved preferentially by goethite. (e) Rehydrated insects affected by manganese oxides. (f) Maximum degree of weathering of Crato insects where oxidizing agents leach the fossil material away leaving behind only their imprint on the sediment.

Supplementary material. To view supplementary material for this article, please visit <https://doi.org/10.1017/S0016756823000043>

Acknowledgements. FIB is grateful for his doctorate scholarship (Coordenação de Aperfeiçoamento de Pessoal de Nível Superior, Brasil – CAPES, process 88882.454892/2019-01). JHS is grateful for the financial support of CNPq no 4/2021 – Research Productivity Grants – PQ, process no. 308064/2021-6. JHS is also grateful for the approved project (FUNCAP) ‘Aid to support research group projects’ Public Notice 07/2021. We acknowledge Dr Charlotte Williams for language revision. The reviews of Jaime Dias and an anonymous are greatly appreciated and improved the quality of the manuscript. Dr Wellington Ferreira da Silva Filho (UFC) has always encouraged our work on the Crato Formation. The authors would like to thank the Central Analítica-UFC/CT-INFRA/MCTI-SISANO/Pró-equipamentos CAPES for the support. We also thank the Federal Police of Brazil

for proactive initiatives which have diminished the illegal international trade of fossils from the Crato Formation.

References

Anderson EP and Smith DM (2017) The same picture through different lenses: quantifying the effects of two preservation pathways on Green River Formation insects. *Paleobiology* **43**, 224–47.
 Arai M and Assine ML (2020) Chronostratigraphic constraints and paleoenvironmental interpretation of the Romualdo Formation (Santana Group, Araripe Basin, Northeastern Brazil) based on palynology. *Cretaceous Research* **116**, 104610. doi: [10.1016/j.cretres.2020.104610](https://doi.org/10.1016/j.cretres.2020.104610).
 Assine ML (2007) Araripe basin. *Boletim de Geociências da Petrobras* **15**, 371–89.
 Assine ML, Perinotto JA, Neumann VH, Custódio MA, Varejão FG and Mescollotti PC (2014) Sequências deposicionais do Andar Alagoas

- (Aptiano superior) da Bacia do Araripe, Nordeste do Brasil. *Boletim de Geociências da Petrobras* **22**, 3–28.
- Barden P and Engel MS** (2021) Fossil social insects. In *Encyclopedia of Social Insects* (ed. CK Starr), pp. 1–21. Cham: Springer International Publishing.
- Barling NT, Heads SW and Martill DM** (2021) Behavioural impacts on the taphonomy of dragonflies and damselflies (Odonata) from the Lower Cretaceous Crato Formation, Brazil. *Palaeoentomology* **4**, 141–55.
- Barling N, Martill DM and Heads SW** (2020) A geochemical model for the preservation of insects in the Crato Formation (Lower Cretaceous) of Brazil. *Cretaceous Research* **116**, 104608. doi: [10.1016/j.cretres.2020.104608](https://doi.org/10.1016/j.cretres.2020.104608).
- Barling N, Martill DM, Heads SW and Gallien F** (2015) High fidelity preservation of fossil insects from the Crato Formation (Lower Cretaceous) of Brazil. *Cretaceous Research* **52**, 605–22.
- Berner RA** (1970) Sedimentary pyrite formation. *American Journal of Science* **268**, 1–23.
- Beurlen KA** (1962) Geologia da Chapada do Araripe. *Anais da Academia Brasileira de Ciências* **34**, 365–70.
- Bezerra FI, da Silva JH, de Paula AJ, Oliveira NC, Paschoal AR, Freire PTC, Viana BC and Mendes M** (2018) Throwing light on an uncommon preservation of Blattodea from the Crato Formation (Araripe Basin, Cretaceous), Brazil. *Revista Brasileira de Paleontologia* **21**, 245–54.
- Bezerra FI, da Silva JH, Miguel EC, Paschoal AR, Nascimento Jr DR, Freire PTC, Viana BC and Mendes M** (2020) Chemical and mineral comparison of fossil insect cuticles from Crato Konservat Lagerstätte, Lower Cretaceous of Brazil. *Journal of Iberian Geology* **46**, 61–76.
- Bezerra FI, Solórzano-Kraemer MM and Mendes M** (2021) Distinct preservational pathways of insects from the Crato Formation, Lower Cretaceous of the Araripe Basin, Brazil. *Cretaceous Research* **118**, 104631. doi: [10.1016/j.cretres.2020.104631](https://doi.org/10.1016/j.cretres.2020.104631).
- Catto B, Jahnert RJ, Warren LV, Varejão FG and Assine ML** (2016) The microbial nature of laminated limestones: lessons from the Upper Aptian, Araripe Basin, Brazil. *Sedimentary Geology* **341**, 304–15.
- Chigira M and Oyama T** (1990) Mechanism and effect of chemical weathering of sedimentary rocks. *Engineering Geology* **55**, 3–14.
- Clapham ME and Karr JA** (2012) Environmental and biotic controls on the evolutionary history of insect body size. *Proceedings of the National Academy of Sciences* **109**, 10927–30.
- Clapham ME, Karr JA, Nicholson DB, Ross AJ and Mayhew PJ** (2016) Ancient origin of high taxonomic richness among insects. *Proceedings of the Royal Society B: Biological Sciences* **283**, 20152476. doi: [10.1098/rspb.2015.2476](https://doi.org/10.1098/rspb.2015.2476).
- Coimbra JC and Freire TM** (2021) Age of the post-rift Sequence I from the Araripe Basin, Lower Cretaceous, NE Brazil: implications for spatio-temporal correlation. *Revista Brasileira de Paleontologia* **24**, 37–46.
- Corecco L, Bezerra FI, Silva Filho WF, Nascimento Júnior DR, da Silva JH and Felix JL** (2022) Petrological meaning of ethnostratigraphic units: laminated limestone of the Crato Formation, Araripe Basin, NE Brazil. *Pesquisas em Geociências* **49**, e121139. doi: [10.22456/1807-9806.121139](https://doi.org/10.22456/1807-9806.121139).
- Cudennec Y and Lecerf A** (2006) The transformation of ferrihydrite into goethite or hematite, revisited. *Journal of Solid State Chemistry* **179**, 716–22.
- Das S and Hendry MJ** (2011) Application of Raman spectroscopy to identify iron minerals commonly found in mine wastes. *Chemical Geology* **290**, 101–8.
- Das S, Hendry MJ and Essilfie-Dughan J** (2011) Transformation of two-line ferrihydrite to goethite and hematite as a function of pH and temperature. *Environmental Science & Technology* **45**, 268–75.
- de Faria DLA and Lopes FN** (2007) Heated goethite and natural hematite: can Raman spectroscopy be used to differentiate them? *Vibrational Spectroscopy* **45**, 117–21.
- Delgado AO, Buck PV, Osés GL, Ghilardi RP, Rangel EC and Pacheco MLAF** (2014) Paleometry: a brand new area in Brazilian science. *Materials Research* **17**, 1434–41.
- Dias JJ and Carvalho IS** (2020) Remarkable fossil crickets preservation from Crato Formation (Aptian, Araripe Basin), a Lagerstätten from Brazil. *Journal of South American Earth Sciences* **98**, 102443. doi: [10.1016/j.jsames.2019.102443](https://doi.org/10.1016/j.jsames.2019.102443).
- Dias JJ and Carvalho IS** (2021) The role of microbial mats in the exquisite preservation of Aptian insect fossils from the Crato Lagerstätte, Brazil. *Cretaceous Research* **130**, 105068. doi: [10.1016/j.cretres.2021.105068](https://doi.org/10.1016/j.cretres.2021.105068).
- Donovan SK** (1991) *The Processes of Fossilization*. London: Belhaven Press.
- Drake H, Tullborg EL and MacKenzie AB** (2009) Detecting the near-surface redox front in crystalline bedrock using fracture mineral distribution, geochemistry and U-series disequilibrium. *Journal of Applied Geochemistry* **24**, 1023–39.
- Du R, Xian H, Wu X, Zhu JH, Wei J, Xing J, Tan W and He H** (2021) Morphology dominated rapid oxidation of framboidal pyrite. *Geochemical Perspectives Letters* **16**, 53–8.
- Duncan IJ and Briggs DEG** (1996) Three-dimensionally preserved insects. *Nature* **381**, 30–1.
- Eggleston CM, Ehrhardt JJ and Stumm W** (1996) Surface structural controls on pyrite oxidation kinetics: an XPS-UPS, STM, and modeling study. *American Mineralogist* **81**, 1036–56.
- Evangelou VP and Zhang YL** (1994) A review: pyrite oxidation mechanisms and acid mine drainage prevention. *Critical Reviews in Environmental Science and Technology* **25**, 141–99.
- Frost RL, Bahfenne S and Graham J** (2008) Infrared and infrared emission spectroscopic study of selected magnesium carbonate minerals containing ferric iron – implications for the geosequestration of greenhouse gases. *Spectrochimica Acta Part A: Molecular and Biomolecular Spectroscopy* **71**, 1610–16.
- Frost RL, Palmer SJ, Spratt HJ and Martens WN** (2011) The molecular structure of the mineral beudantite $\text{PbFe}_3(\text{AsO}_4, \text{SO}_4)_2(\text{OH})_6$ – implications for arsenic accumulation and removal. *Journal of Molecular Structure* **988**, 52–8.
- Frost RL, Scholz R and López A** (2016) A Raman and infrared spectroscopic study of the phosphate mineral laueite. *Vibrational Spectroscopy* **82**, 31–6.
- Frost RL and Xi Y** (2012) A vibrational spectroscopic study of the phosphate mineral wardite $\text{NaAl}_3(\text{PO}_4)_2(\text{OH})_4 \cdot 2(\text{H}_2\text{O})$. *Spectrochimica Acta Part A: Molecular and Biomolecular Spectroscopy* **93**, 155–63.
- Giovanoli R** (1980) On natural and synthetic manganese nodules. In *Geology and Geochemistry of Manganese* (eds IM Varentsov and GY Grasselly), pp. 191–9. Stuttgart: Schweizerbart.
- Greenwalt DE, Rose TR, Siljeström SM, Goreva YS, Constenius KN and Wingerath JG** (2015) Taphonomy of the fossil insects of the middle Eocene Kishenehn Formation. *Acta Palaeontologica Polonica* **60**, 931–47.
- Gu X, Heaney PJ, Reis FDA and Brantley SL** (2020) Deep abiotic weathering of pyrite. *Science* **370**, eabb8092. doi: [10.1126/science.abb8092](https://doi.org/10.1126/science.abb8092).
- Gunasekaran S and Anbalagan G** (2007) Spectroscopic study of phase transitions in dolomite mineral. *Journal of Raman Spectroscopy* **38**, 846–52.
- Hassan MF, Rahman MM, Guo ZP, Chen ZX and Liu HK** (2010) Solvent-assisted molten salt process: a new route to synthesise $\alpha\text{-Fe}_2\text{O}_3/\text{C}$ nanocomposite and its electrochemical performance in lithium-ion batteries. *Electrochimica Acta* **55**, 5006–13.
- Heimhofer U, Ariztegui D, Lenniger M, Hesselbo SP, Martill DM and Rios-Netto AM** (2010) Deciphering the depositional environment of the laminated Crato fossil beds (Early Cretaceous, Araripe Basin, North-eastern Brazil). *Sedimentology* **57**, 677–94.
- Heingård M, Sjövall P, Schultz BP, Sylvestersen RL and Lindgren J** (2022) Preservation and taphonomy of fossil insects from the earliest Eocene of Denmark. *Biology* **11**, 395. doi: [10.3390/biology11030395](https://doi.org/10.3390/biology11030395).
- Henwood AA** (1992) Exceptional preservation of dipteran flight muscle and the taphonomy of insects in amber. *Palaos* **7**, 203–12.
- Henwood AA** (1993) Ecology and taphonomy of Dominican Republic amber and its inclusions. *Lethaia* **26**, 237–45.
- Iniesto M, Gutiérrez-Silva P, Dias JJ, Carvalho IS, Buscalioni AD and López-Archilla AI** (2021) Soft tissue histology of insect larvae decayed in laboratory experiments using microbial mats: taphonomic comparison with Cretaceous fossil insects from the exceptionally preserved biota of Araripe, Brazil. *Palaeogeography, Palaeoclimatology, Palaeoecology* **564**, 110156. doi: [10.1016/j.palaeo.2020.110156](https://doi.org/10.1016/j.palaeo.2020.110156).
- Jerz JK and Rimstidt JD** (2004) Pyrite oxidation in moist air. *Geochimica et Cosmochimica Acta* **68**, 701–14.

- Jorgensen FRA and Moyle FJ** (1982) Phases formed during the thermal analysis of pyrite in air. *Journal of Thermal Analysis and Calorimetry* **25**, 473–85.
- Julien C, Massot M and Poinsignon C** (2004) Lattice vibrations of manganese oxides. *Spectrochimica Acta Part A: Molecular and Biomolecular Spectroscopy* **60**, 689–700.
- Karr JA and Clapham ME** (2015) Taphonomic biases in the insect fossil record: shifts in articulation over geologic time. *Paleobiology* **41**, 16–32.
- Kribe B** (1975) The origin of framboidal pyrite as a surface effect of sulphur grains. *Mineralium Deposita* **10**, 389–96.
- Labandeira CC** (2019) The fossil record of insect mouthparts: innovation, functional convergence, and associations with other organisms, In *Insect Mouthparts: Form, Function, Development and Performance* (ed. HW Krenn), pp. 567–671. Cham: Springer.
- Labandeira CC, Kustatscher E and Wappler T** (2016) Floral assemblages and patterns of insect herbivory during the Permian to Triassic of northeastern Italy. *PLoS One* **11**, e0165205. doi: [10.1371/journal.pone.0165205](https://doi.org/10.1371/journal.pone.0165205).
- Legodi MA and de Waal D** (2007) The preparation of magnetite, goethite, hematite and maghemite of pigment quality from mill scale iron waste. *Dyes and Pigments* **74**, 161–8.
- Li S and Hihara LH** (2015) A micro-Raman spectroscopic study of marine atmospheric corrosion of carbon steel: the effect of akaganeite. *Journal of the Electrochemical Society* **162**, 495–502.
- Marques FO, Nogueira FCC, Bezerra FHR and de Castro DL** (2014) The Araripe Basin in NE Brazil: an intracontinental graben inverted to a high-standing horst. *Tectonophysics* **630**, 251–64.
- Marshall CP and Marshall AO** (2013) Raman hyperspectral imaging of microfossils: potential pitfalls. *Astrobiology* **13**, 920–31.
- Martill DM, Bechly G and Loveridge RF** (2007) *The Crato Fossil Beds of Brazil – Window Into an Ancient World*. Cambridge: Cambridge University Press.
- Martínez-Delclòs X, Briggs DEG and Peñalver E** (2004) Taphonomy of insects in carbonates and amber. *Palaeogeography, Palaeoclimatology, Palaeoecology* **203**, 19–64.
- Matos RMD** (1992) The northeast Brazilian rift system. *Tectonics* **114**, 766–91.
- McNamara ME** (2013) The taphonomy of colour in fossil insects and feathers. *Palaeontology* **56**, 557–75.
- McNamara ME, Briggs DEG and Orr PJ** (2012) The controls of the preservation of structural color in fossil insects. *Palaio* **27**, 443–54.
- McNamara ME, Briggs DEG, Orr PJ, Wedmann S, Noh H and Cao H** (2011) Fossilized biophotonic nanostructures reveal the original colors of 47-million-year-old moths. *PLoS Biology* **9**, e1001200. doi: [10.1371/journal.pbio.1001200](https://doi.org/10.1371/journal.pbio.1001200).
- Melo RM, Guzmán J, Almeida-Lima D, Piovesan EK, Neumann VHML and Sousa AJ** (2020) New marine data and age accuracy of the Romualdo Formation, Araripe Basin, Brazil. *Scientific Reports* **10**, 15779. doi: [10.1038/s41598-020-72789-8](https://doi.org/10.1038/s41598-020-72789-8).
- Miranda TS, Barbosa JA, Gomes IF, Santos RF, Neumann VH, Matos GC, Guimarães L, Queiroz RM and Alencar M** (2012) Applying scanline techniques to geological/geomechanical modeling of fracturing systems in carbonate and evaporite deposits from Araripe Basin, NE Brazil. *Boletim de Geociências da Petrobras* **20**, 305–26.
- Miranda T, Barbosa JA, Gomes IF, Soares A, Santos RFVC, Matos GC, McKinnon EA, Neumann VH and Marrett RA** (2016) Petrophysics and petrography of Aptian tight carbonate reservoir, Araripe Basin, NE Brazil. In *78th European Association of Geoscientists and Engineers Conference and Exhibition*. Vienna: European Association of Geoscientists and Engineers.
- Miranda TS, Santos RF, Barbosa JA, Gomes IF, Alencar ML, Correia OJ, Falcão TC, Gale J and Neumann VH** (2018) Quantifying aperture, spacing and fracture intensity in a carbonate reservoir analogue: Crato Formation, NE Brazil. *Marine and Petroleum Geology* **97**, 556–67.
- Mohapatra M, Behera D, Layek S, Anand S, Verma HC and Mishra BK** (2011) Influence of Ca ions on surfactant directed nucleation and growth of nano structured iron oxides and their magnetic properties. *Crystal Growth & Design* **12**, 18–28.
- Musić S, Krehula S, Popović S and Skoko Ž** (2003) Some factors influencing forced hydrolysis of FeCl₃ solutions. *Materials Letters* **57**, 1096–102.
- Nicholson DB, Mayhew PJ and Ross AJ** (2015) Changes to the fossil record of insects through fifteen years of discovery. *PLoS One* **10**, e0128554. doi: [10.1371/journal.pone.0128554](https://doi.org/10.1371/journal.pone.0128554).
- Nordstrom DK** (1982) Aqueous pyrite oxidation and the consequent formation of secondary iron minerals. In *Acid Sulfate Weathering* (eds JA Kittrick, DS Fanning and LR Hossner), pp. 37–56. SSSA Special Publication 10. Madison: Soil Science Society of America.
- Ohfuji H and Rickard D** (2005) Experimental syntheses of framboids – a review. *Earth-Science Reviews* **71**, 147–70.
- Osés GL, Petri S, Becker-Kerber B, Romero GR, Rizzutto MA, Rodrigues F, Galante D, da Silva TF, Curado JF, Rangel EC, Ribeiro RP and Pacheco MLAF** (2016) Deciphering the preservation of fossil insects: a case study from the Crato Member, Early Cretaceous of Brazil. *PeerJ* **4**, e2756. doi: [10.7717/peerj.2756](https://doi.org/10.7717/peerj.2756).
- Pal B and Sharon M** (2000) Preparation of iron oxide thin film by metal organic deposition from Fe (III)-acetylacetonate: a study of photocatalytic properties. *Thin Solid Films* **379**, 83–8.
- Pan Y, Sha J and Fürsich FT** (2014) A model for organic fossilization of the early Cretaceous Jehol lagerstätte based on the taphonomy of *Ephemeroptera trisetalis*. *Palaio* **29**, 363–77.
- Prado G, Arthuzzi JCL, Osés GL, Callo F, Maldanis L, Sucerquia P, Becker-Kerber B, Romero GR, Quiroz-Valle FR and Galante D** (2021) Synchrotron radiation in palaeontological investigations: examples from Brazilian fossils and its potential to South American palaeontology. *Journal of South American Earth Sciences* **108**, 102973. doi: [10.1016/j.jsames.2020.102973](https://doi.org/10.1016/j.jsames.2020.102973).
- Pugh CE, Hossner LR and Dixon JB** (1984) Oxidation rate of iron sulfides as affected by surface area, morphology, oxygen concentration and autotrophic bacteria. *Soil Science* **137**, 309–14.
- Putnis A** (2009) Mineral replacement reactions. *Reviews in Mineralogy and Geochemistry* **70**, 87–124.
- Raji M, Quass AK and Bouhfid R** (2020) Effects of bleaching and functionalization of kaolinite on the mechanical and thermal properties of polyamide 6 nanocomposites. *RSC Advances* **10**, 4916–26.
- Rimstidt JD and Vaughan DJ** (2003) Pyrite oxidation: a state-of-the-art assessment of the reaction mechanism. *Geochimica et Cosmochimica Acta* **67**, 873–80.
- Rodriguez-Blanco JD, Shaw S and Benning LG** (2011) The kinetics and mechanisms of amorphous calcium carbonate (ACC) crystallization to calcite, via vaterite. *Nanoscale* **3**, 265–71.
- Schachat SR and Labandeira CC** (2021) Are insects heading toward their first mass extinction? Distinguishing turnover from crises in their fossil record. *Annals of the Entomological Society of America* **114**, 99–118.
- Schaufuß AG, Nesbitt HW, Kartio I, Laajalehto K, Bancroft GM and Szargan R** (1998a) Reactivity of surface chemical states on fractured pyrite. *Surface Science* **411**, 321–8.
- Schaufuß AG, Nesbitt HW, Kartio I, Laajalehto K, Bancroft GM and Szargan R** (1998b) Incipient oxidation of fractured pyrite surfaces in air. *Journal of Electron Spectroscopy and Related Phenomena* **96**, 69–82.
- Schiffbauer JD, Xiao S, Cai Y, Wallace AF, Hua H, Hunter J, Xu H, Peng Y and Kaufman AJ** (2014) A unifying model for Neoproterozoic–Palaeozoic exceptional fossil preservation through pyritization and carbonaceous compression. *Nature Communications* **5**, 5754. doi: [10.1038/ncomms6754](https://doi.org/10.1038/ncomms6754).
- Schwertmann U** (1988) Goethite and hematite formation in the presence of clay minerals and gibbsite at 25 °C. *Soil Science Society of America Journal* **52**, 288–91.
- Singer PC and Stumm W** (1970) Acid mine drainage-rate determining step. *Science* **167**, 1121–3.
- Smith DM** (2012) Exceptional preservation of insects in lacustrine environments. *Palaio* **27**, 346–53.
- Smith DM, Cook A and Nufio CR** (2006) How physical characteristics of beetles affect their fossil preservation. *Palaio* **21**, 305–10.
- Smith DM and Moe-Hoffman AP** (2007) Taphonomy of Diptera in lacustrine environments: a case study from Florissant Fossil Beds, Colorado. *Palaio* **22**, 623–9.

- Thoene-Henning J, Smith DM, Nufio CR and Meyer HW** (2012) Depositional setting and fossil insect preservation: a study of the late Eocene Florissant Formation, Colorado. *Palaios* **27**, 481–8.
- Tian Q, Wang S, Yang Z, McNamara ME, Benton MJ and Jiang B** (2020) Experimental investigation of insect deposition in lentic environments and implications for formation of *Konservat Lagerstätten*. *Palaeontology* **63**, 565–78.
- Tiwari I, Singh M, Pandey CM and Sumana G** (2015) Electrochemical genosensor based on graphene oxide modified iron oxide–chitosan hybrid nanocomposite for pathogen detection. *Sensors & Actuators, B: Chemical* **206**, 276–83.
- Varejão FG, Warren LV, Simões MG, Buatois LA, Mángano MG, Bahniuk AMR and Assine ML** (2021) Mixed siliciclastic-carbonate sedimentation in an evolving epicontinental sea: Aptian record of marginal marine settings in the interior basins of north-eastern Brazil. *Sedimentology* **68**, 2125–64.
- Varejão FG, Warren LV, Simões MG, Fürsich FT, Matos SA and Assine ML** (2019) Exceptional preservation of soft tissues by microbial entombment: insights into the taphonomy of the Crato *Konservat-Lagerstätte*. *Palaios* **34**, 331–48.
- Wang B, Zhao F, Zhang H, Fang Y and Zheng D** (2012) Widespread pyritization of insects in the Early Cretaceous Jehol biota. *Palaios* **27**, 707–11.
- Warren LV, Varejão FG, Quaglio F, Simões MG, Fürsich FT, Poiré DG, Catto B and Assine ML** (2017) Stromatolites from the Aptian Crato Formation, a hypersaline lake system in the Araripe Basin, northeastern Brazil. *Facies* **63**, 3. doi: [10.1007/s10347-016-0484-6](https://doi.org/10.1007/s10347-016-0484-6).
- Wildman RA, Berner RA, Petsch ST, Bolton EW, Eckert JO, Mok U and Evans JB** (2004) The weathering of sedimentary organic matter as a control on atmospheric O₂: I. Analysis of a black shale. *American Journal of Science* **304**, 234–49.
- Zhehikhin VV** (2002) Pattern of insect burial and conservation. In *History of Insects* (eds AP Rasnitsyn and DLJ Quicke), pp. 17–63. Dordrecht: Springer.
- Zuo J, Zhao X, Wu R, Du G, Xu C and Wang C** (2003) Analysis of the pigments on painted pottery figurines from the Han Dynasty's Yangling Tombs by Raman microscopy. *Journal of Raman Spectroscopy* **34**, 121–5.